GEOPHYSICAL RESEARCH LETTERS, VOL. 11, NO. 8, PAGES 799-801, AUGUST 1984

SEA SURFACE DYNAMIC HEIGHT TOPOGRAPHY AND THE NORTH EQUATORIAL COUNTERCURRENT AS INFERRED FROM A LINEAR MODEL

Yves du Penhoat[1] and Anne-Marie Treguier

Antenne ORSTOM, Centre Oceanologique de Bretagne, Brest, France

Abstract. Hellerman and Rosenstein's (1983) climatological winds are used to force a linear, continuously stratified model of the tropical Atlantic. The dynamic height topography relative to 500 meters is compared with available data. Special attention is paid to the computed North Equatorial Countercurrent. We conclude that most of the observed seasonal variations can be explained using simple linear theory.

Introduction

The FOCAL and SEQUAL experiments are designed to understand the seasonal variability of the tropical Atlantic. In this ocean, the seasonal signal is stronger than the interannual mainly because of the wind cycle. As shown in Merle (1980), heat fluxes through the surface cannot explain more than 10% of heat content variations on a seasonal time scale. Then we assume that, at sufficiently low frequency, the ocean response is essentially a dynamic response to wind forcing and because of equatorial wave guide properties, strong seasonal variations are expected.

Many of the observed changes can be explained by linear theory (e.g., Busalacchi and Picaut, 1983). Here we describe an experiment forcing a linear continuously stratified model with climatological winds (Hellerman and Rosenstein, 1983). The vertical structure is solved in terms of vertical normal modes with a background density profile computed from many observations along the equator. The horizontal structure is numerically calculated using the properties of the low frequency equatorial motions. This fast and efficient numerical procedure (Patton, 1981) permits a time step of order 10 days (instead of hours as in usual numerical models) and makes it a very efficient tool for long period experiments. Damping in the model is caused by Rayleigh friction and Newtonian cooling at the same decay rate and increases with model number. With this simple assumption the solution is still separable into vertical modes.

As the oceanic response is influenced by more than a single mode, we sum over the first nine ones to obtain the vertical structure. Higher modes are not a significant part of the solution, as we are interested in the upper ocean (down to 600 meters). By solving the vertical structure, we are able to compute the dynamic height topography relative to 500 meters, which is directly comparable to historical data, and also to data given by tide gauges. Furthermore, it will be comparable to synoptic sea surface topography pictures given by satellite altimetry.

Results

We shall focus the present note on the dynamic height field relative to 500 meters using the relation:

$$d = do + \sum_{n=1}^{N} P_n \, d_n \qquad (1)$$

Where d is the dynamic height anomaly, do is a constant depending on the density profile and the reference density, $P_n(x,y,t)$ is the sea surface pressure field associated with the nth baroclinic mode and d_n depends on each individual mode n. Figures 1-3 are obtained by summing over three modes. Comparing with a sum of nine modes, 95% of the dynamic height signal at the equator and almost 100% as we move polewards are explained by the first three modes. This can be understood by considering that 50% of the wind stress projects on these modes, that higher modes are more heavily damped, and that between 0 and 500 meters the gravest modes dominate the solution.

Figures 1a and 1b show a good qualitative agreement between historical data and the model results for the amplitude of the annual signal. The phase diagrams (not shown) reproduce the regions of rapid phase variations observed, with the "pivot" zone near 25° W at the equator and the pivot line in a meridional plane farther north. The annual amplitude is very well reproduced in the eastern part of the basin. The model also shows the importance of the semiannual signal in that area.

Along the equator the response is directly related to the zonal wind stress, as shown by time longitude plots (Figure 2). The dynamic height gradient is minimum in March-April when the zonal wind stress is the weakest. The wind begins to increase first in the east and then to the west (Picaut, 1983). Similarly the dynamic height gradient reaches its maximum first in the east (July) and then in the west (September). The slope gets steeper in the west corresponding to a stronger wind stress there. We conclude that the computed pattern is a typical periodic response as described by Cane and Sarachik (1981), resulting from multiple reflexions and interferences of low frequency waves (equatorial Kelvin waves and long Rossby waves). Away from the equator, the dynamic balance changes; the equatorial Kelvin wave and the gravest meridional Rossby modes no longer matter. Higher Rossby modes and Ekman pumping dominate the solution; the dynamic height will not be rapidly adjusted to the forcing on the basin scale.

In the northeast part of the basin, centered

[1]Presently at Centre de Recherches Oceanographiques Dakar Thiaroye, Senegal.

Paper number 4L6119.
0094-8276/84/004L-6119$03.00

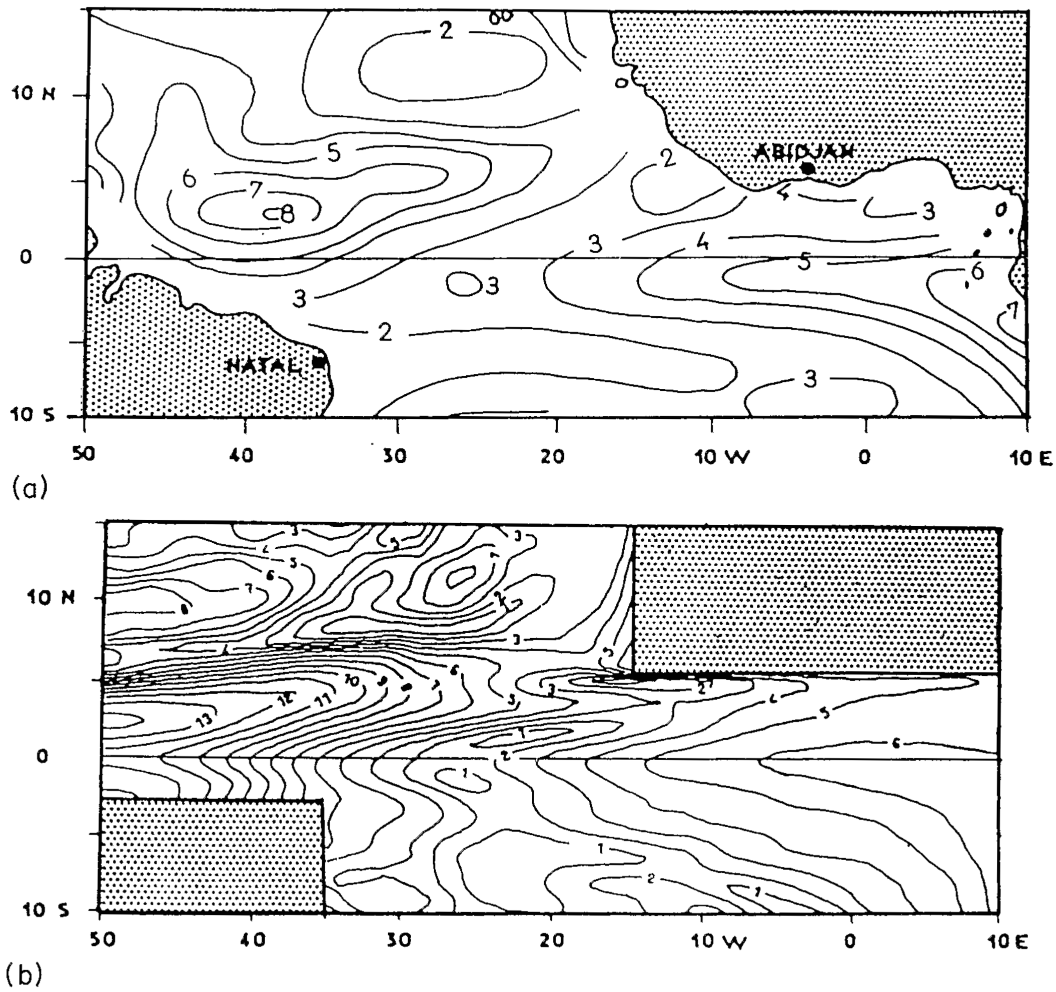

Fig. 1. Annual amplitude of the dynamic height topography (in dyn. cm). (a) Observations (courtesy of S. Arnault and J. Merle). (b) model results.

at 25°W, 12°N, there is a region of minimum annual amplitude of dynamic height (minimum of 2 dyn. cm, see Figure 1). This feature, which very closely corresponds to historical data, is the so called Guinea dome which is characterized by a shallow thermocline and is more clearly evident in northern summer when the ITCZ straddles this area (Voituriez, 1981). It appears clearly in our calculation in August and reaches its minimum of 68 dyn. cm in September. If the wind stress

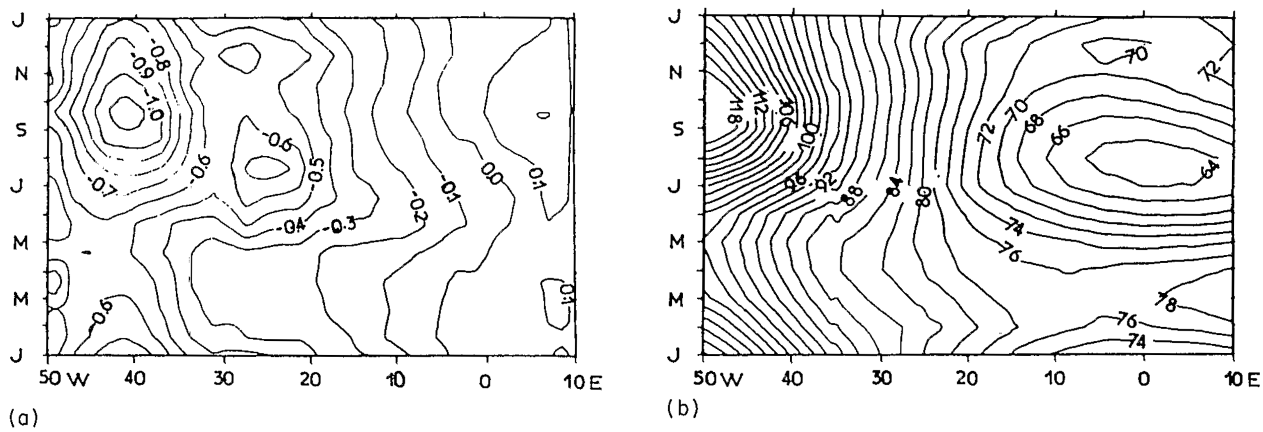

Fig. 2.(a) Time longitude plot of zonal wind stress along the equator, averaged between 1°N and 1°S (dynes/cm^2). From Hellerman data. (b) Time longitude plot of computed dynamic height along the equator, averaged between 1°N and 1°S (dyn. cm).

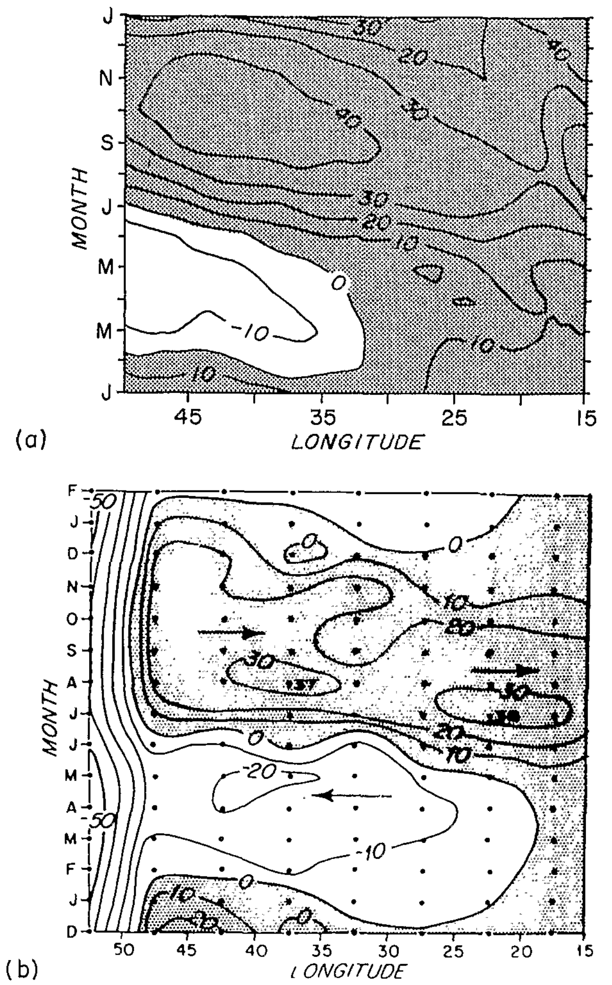

Fig. 3.(a) Time longitude plot of computed zonal component of the NECC averaged between 5°N and 8°N (cm/s). (b) Time longitude plot of zonal velocity of the NECC averaged between 5°N and 8°N (cm/s) from ship drift data (courtesy of P. Richardson).

curl is upwelling favorable in this area at this time of the year, the influence of higher Rossby modes is also important and can be seen in the bending of dynamic height contours, a characteristic of Rossby mode radiation.

One of the major components of the surface current system associated with the ridge of dynamic height around 4°-10°N is the eastward North Equatorial Countercurrent (NECC). It is characterized by strong seasonal variations associated with wind forcing fluctuations. Its mean position is closely related to the mean position of the ITCZ. It is stronger in northern summer with a maximum meridional extension.

As opposed to the dynamic height topography, the contribution of higher modes is necessary to describe the current field, and we sum over nine modes to get the solution. However, the first three modes account for almost 90% of the seasonal variations of the NECC. Figure 3a shows model results for the NECC compared to observations (Figure 3b, courtesy of P. Richardson), averaged between 5° and 8°N. The quantitative agreement is very good, except in the west as the model does not treat the western boundary layer. The reversal event in northern spring is reproduced but with a smaller longitudinal extension than in observations. Every mode but the first reverses and higher modes ($n \geq 3$) are an important part of the solution at that time.

The establishment of the NECC starts in the east around 20 west and propagates westward, a feature present in ship drift data (Richardson, personal communication). Comparison between the NECC and the meridional dynamic height gradient tends to support the geostropic balance for the NECC.

Conclusion

With a simple linear stratified model we are able to describe the principal characteristics of the tropical Atlantic circulation. The model equations filter out high frequency motions and short Rossby waves. The vertical structure is solved in terms of baroclinic modes. The model calculates dynamic height and thus allows a quantitative comparison with historical data. The main observed features of dynamic height as well as its seasonal variations are essentially a linear response to wind forcing in the equatorial Atlantic.

The model seems to reproduce rather well the seasonal cycle of zonal currents, and a few degrees away from the equator, current speeds are in good agreement with observations. This is particularly true for the NECC, for both the mean and time variations.

References

Busalacchi, A.J. and J. Picaut, Seasonal variability from a model of the tropical Atlantic Ocean, J. Phys. Oceanogr., 13 1564-1588, 1983.

Cane, M.A. and E.S. Sarachik, The response of a linear baroclinic equatorial ocean to periodic forcing, J. Mar. Res., 39, 652-693, 1981.

Hellerman, S. and Rosenstein, M., Normal monthly wind stress over the world ocean with error estimates, J. Phys. Oceanogr., 13, 1093-1104, 1983.

Merle, J., Seasonal heat budget in the equatorial Atlantic Ocean, J. Phys. Oceanogr., 11, 1443-1451, 1980.

Patton, R.J., A numerical model of equatorial waves with application to the seasonal upwelling in the Gulf of Guinea, M.S. thesis, 120 pp, Mass. Inst. of Technol., Cambridge, 1981.

Picaut, J. Propagation of the seasonal upwelling in the eastern equatorial Atlantic, J. Phys. Oceanogr., 13, 18-37, 1983.

Voituriez, B., Les sous courants equatoriaux Nord et Sud et la Formation des domes thermiques tropicaux, Oceanolog. Acta., 4, 497-506, 1981.

Y du Penhoat, Centre ORSTOM, B.P. 1386, Dakar, Senegal.

(Received March 14, 1984;
revised May 24, 1984;
accepted June 4, 1984.)